Autophagy at Crossroads: Modulating Responses to Combined Heat Stress and Bacterial Infection.

Short title: Autophagy: Autophagy at the Nexus of Combined Biotic and Abiotic Stresses

Heike Seybold[#]*, Ella Katz, Yoram Soroka and Tamar Avin-Wittenberg*

The Hebrew University of Jerusalem, Department of Plant and Environmental Sciences, Alexander Silberman Institute of Life Sciences, Edmond Safra Campus, Jerusalem, Israel.

Current address: Federal Research Centre for Cultivated Plants, Julius Kühn-Institut, Institute for Strategies and Technology Assessment, Kleinmachnow, Germany.

* Corresponding authors
tamar.avin-wittenberg@mail.huji.ac.il
heike.seybold@mail.huji.ac.il

Abstract

Plants face diverse stresses in natural environments, necessitating complex responses for survival. Abiotic and biotic stress responses are typically counteractive, posing challenges for breeding crops resilient to multiple stresses. Autophagy, a cellular transport process, plays a vital role in plant stress response, facilitating the degradation of cellular components and enabling nutrient recycling. Here, we asked what the role of autophagy is in combined abiotic (heat) and biotic (bacterial infection by *Xanthomonas campestris* pv. *vesicatoria*) stress. We introduce a conceptual framework based on assays monitoring autophagy activation, bacterial infection, and metabolic profiling.

We observed that heat stress facilitates bacterial growth in an autophagy-dependent manner. Bacterial effectors facilitate this phenomenon. We also demonstrate the engagement of the autophagy-related 8 (ATG8) protein family members in stress-specific activation. Metabolic profiling highlights effector-dependent shifts in nutrient availability during stress, influencing bacterial performance. Our study challenges the assumption that combined stresses are simply the sum of individual responses as exemplified by activation of the autophagic pathway. Instead, it establishes autophagy as a link connecting environmental factors and plant-microbe interactions. Insights for our study can present a novel perspective for designing strategies to enhance crop resilience in the face of multifaceted challenges.

Introduction

Field-grown plants face many stresses, both abiotic (e.g., drought, temperature) and biotic (e.g., pathogens), requiring intricate physiological and molecular strategies for survival. Understanding these strategies has become more urgent due to climate change and the spread of new pests and diseases linked with these changes (Luck et al., 2011, Cavicchioli et al., 2019). Moreover, the nature and severity of stresses encountered by crops are predicted to worsen (Bebber, 2015, Hey et al., 2009). Abiotic and biotic stress responses are typically perceived to be counteractive, thus posing a significant challenge for breeding crops resilient to multiple stresses (Zhang and Sonnewald, 2017). Despite their distinct nature, there are intriguing similarities in the signaling patterns of biotic and abiotic stress responses, such as changes in phytohormone levels, calcium influx, reactive oxygen species (ROS) production, and activation of specific transcription factors (Atkinson and Urwin, 2012, Fraire-Velazquez et al., 2011, Jones and Dangl, 2006, Glazebrook, 2005, Dodds and Rathjen, 2010, Islam et al., 2018, Ohama et al.,

2017, Zhu, 2016). Another common feature of these stresses is the redirection of energy resources from growth to stress responses (Signorelli et al., 2019).

Autophagy, a conserved eukaryotic mechanism, is vital for the recycling of cellular components and energy sourcing (Yang and Klionsky, 2009, Feng et al., 2013, Masclaux-Daubresse et al., 2020, Liu and Bassham, 2012). In plants, three types of autophagy have been described: Micro-, Macro-, and Megautophagy (Liu and Bassham, 2012, van Doorn and Papini, 2014, Marshall and Vierstra, 2018). Macroautophagy (hereafter called autophagy) is extensively studied and involves the formation of cytosolic double-membrane vesicles called autophagosomes. Autophagosomes deliver cytosolic cargo, which can be randomly (bulk autophagy) or selectively acquired (selective autophagy), to the vacuole for degradation (Liu and Bassham, 2012). Though autophagy functions in both plant biotic and abiotic stress responses (Signorelli et al., 2019), little is known regarding its role in combined stresses. Here, we focused on the role of autophagy in the combination of heat stress (abiotic stress) and bacterial infection (biotic stress).

Autophagy progression is divided into distinct steps and, in plants, involves more than 40 autophagy-related (ATG) proteins (Liu and Bassham, 2012, Yang and Klionsky, 2010, Chen and Klionsky, 2011, Chung, 2019, Wang et al., 2011). *ATG* genes are regulated on a transcriptional level, and *ATG* transcript availability and timing are critical for an appropriate stress response (Magen et al., 2022). Plant transcription factors were shown to confer abiotic stress resistance by inducing *ATG* gene expression and, consequently, autophagy (Wang et al., 2015, Zhu et al., 2018). The WRKY transcription factor family is particularly interesting regarding combined stress. WRKY33 induces autophagy in response to both abiotic and biotic stresses by activating the transcription of *ATG5* and *ATG7*. It is involved in heat tolerance in different plant species and, in addition to *ATG* genes, induces the expression of defense-related genes in *Arabidopsis thaliana* (Arabidopsis) (Lai et al., 2011, Schmidt et al., 2019, Mao et al., 2011, Lippok et al., 2007, Zhou et al., 2014, Zheng et al., 2006). Arabidopsis knockout mutants of *ATG* genes (*atg* mutants) are hypersensitive to different stresses, while overexpression of *ATG* genes improves plant fitness and performance (Liu and Bassham, 2012, Slavikova et al., 2008, Minina et al., 2018, Magen et al., 2022, Zhang et al., 2020).

Heat can have cytotoxic effects resulting in cellular metabolism and homeostasis perturbations due to protein denaturation and aggregation. Plant autophagy can remove heat-induced protein aggregates (Baxter et al., 2013, Zhou et al., 2013, Zhou et al., 2014). In addition, Neighbor Of BRCA1 (NBR1) mediates the selective degradation of proteins by autophagy to play a crucial role in the recovery from heat stress by regulating heat stress memory (Thirumalaikumar et al.,

2020). NBR1 recruits cargo to the autophagosome by interaction with ATG8, a small ubiquitin-like protein, which undergoes lipidation by Phosphatidylethanolamine upon autophagy induction (Svenning et al., 2011, Zhou et al., 2013). The inner autophagosomal membrane, associated proteins (ATG8, NBR1), and cargo undergo degradation within the vacuole. The number of ATG8 isoforms varies among plant species, expanding from one isoform in algae to multiple isoforms in vascular plants (Zess et al., 2019). Notably, ATG8 exhibits a non-canonical function in response to heat stress, aiding the Golgi apparatus reassembly in Arabidopsis after acute heat stress (Zhou et al., 2023).

The role of autophagy in biotic stress response is more complicated and depends on the pathogen's lifestyle (Sertsuvalkul et al., 2022). Bacterial plant pathogens, residing extracellularly, employ a type 3 secretion system (T3SS) to deliver effectors into the plant cell, manipulating cellular processes, including autophagy, for their benefit (Üstün et al., 2016, Lal et al., 2020, Leong et al., 2022b). NBR1-mediated selective autophagy can antagonize the effector-driven virulence (Leong et al., 2022b, Ustun et al., 2018). Besides bacterial pathogens, the oomycete *Phytophthora infestans* inhibits autophagy through effectors, countered by NBR1-mediated selective autophagy (Pandey et al., 2021, Dagdas et al., 2016, Dagdas et al., 2018). In addition, overexpression of *ATG5* or *ATG7* increased resistance against the necrotrophic fungal pathogen *Alternaria brassicicola*, and other examples support a positive role for autophagy in defense responses against necrotrophic plant pathogens (Minina et al., 2018, Lai et al., 2011, Lenz et al., 2011, Patel and Dinesh-Kumar, 2008). In line with these findings, autophagy plays a negative role in defense responses against obligate biotrophic pathogens (Wang et al., 2011). In contrast to oomycetes and bacterial pathogens, plant viruses, present intracellularly, are removed directly through NBR1-dependent selective autophagy (Hafren et al., 2017, Hafren et al., 2018).

Despite the significance of combined stresses in real-world natural and agricultural settings, research on their impact, particularly involving autophagy, remains limited. Understanding how plants respond to combined stresses is crucial for ensuring crop fitness and productivity in the face of climate change. The interaction between plant stress responses can be synergistic. Still, in most cases, responses to combined stresses differ significantly from those to single stresses (Rasmussen et al., 2013, Pandey et al., 2015, Ramegowda and Senthil-Kumar, 2015, Zhang and Sonnewald, 2017). Plant autophagy as a pathway involved in various stress responses has an exciting potential to increase plant tolerance towards combined stress scenarios with broad agricultural implications. Here, we investigate the pivotal role of autophagy in orchestrating the response to combined stresses. We chose a dual stress paradigm involving elevated temperature

118 followed by infection with the bacterial pathogen *Xanthomonas campestris* pv. *vesicatoria*
119 (*Xcv*), the causal agent of bacterial spot disease on pepper and tomato. Autophagy was shown
120 to contribute to plant defense against *Xanthomonas* pathogens, while *Xcv* targets autophagy to
121 inhibit appropriate defense responses (Yan et al., 2017, Leong et al., 2022b).
122

123 **Materials and Methods**

124 **Biological material and growth conditions**

125 *Nicotiana benthamiana* mutant line Δ*roq1* was kindly provided by Johannes Stuttmann (CEA,
126 France; (Grutzner et al., 2021)). Transient expression constructs were kindly provided by Yasin
127 Dagdas (Gregor Mendel Institute, Austria; GFP-*StATG8* isoforms) and Elena Minina (Swedish
128 University of Agricultural Sciences, Sweden; *AtATG7*). *Xanthomonas campestris* pv.
129 *vesicatoria* (*Xcv*) strains 85-10 and 85-10 Δ*hrcV* were kindly provided by Guido Sessa (Tel
130 Aviv University, Israel).
131 *Solanum lycopersicum* M82 and *N. benthamiana* were grown under a 16h light/8h darkness
132 cycle (long day, LD), 22 °C. Tomato plants were used for stress experiments at the age of five
133 weeks, tobacco plants were transformed and subsequently stressed at an age of approximately
134 four weeks. All plant were grown in a mixture of commercial plant soil, perlit, and vermiculite
135 (2:1:1).

136 **Stress treatments**

137 To induce carbon starvation, plant trays were covered with aluminum foil for three days but
138 kept in the same climate chamber as control plants without carbon starvation. For biotic stress
139 treatments, *Xcv* suspensions of OD_{600} 0.2 in 10 mM $MgCl_2$ were pressure-infiltrated into leaf
140 tissue of *N. benthamiana* using a needle-less syringe. Plants were placed into a Percival
141 chamber at 22 °C (control temperature) for 6 h. For heat stress treatments, plants were placed
142 into a second Percival chamber and subjected to 40 °C for 6 h.

143 **Bacterial growth assay**

144 *Xcv* was grown in NYGB medium at 28 °C overnight. For measuring bacterial growth, leaves
145 of five-week old tomato plants or four-week old tobacco plants were pressure-infiltrated with
146 *Xcv* OD_{600} 0.0004 in 10 mM $MgCl_2$ with or without 5 mM 3-Methyladenine (3-MA) using a
147 needle-less syringe. Leaf disk samples were taken immediately after infiltration of an
148 independent set of plants to ensure equal infiltration densities. To check bacterial performance,

149 leaf disk samples were taken three days after inoculation. Bacterial growth was monitored by
150 serial dilution plating of ground leaf discs.

151 **Transient expression in tobacco**

152 To study the stress specificity of ATG8 isoforms, *Agrobacterium tumefaciens* strain
153 GV3101::pMP90 was transformed by electroporation with constructs of N-terminally GFP-
154 tagged versions of all seven *St*ATG8 isoforms (Zess et al., 2019), respectively. For transient
155 expression in *N. benthamiana* Δ*roq1* plants, bacteria were grown in LB medium at 28 °C
156 overnight, resuspended in infiltration buffer (10 mM MES, pH 5.7; 10 mM $MgCl_2$; 150 µM
157 Acetosyringone), adjusted to OD_{600} 0.5 and incubated for 2 hours at room temperature. The
158 bacteria were subsequently pressure-infiltrated into *N. benthamiana* leaf tissue using a needle-
159 less syringe. After an initial phase of 18 h under LD conditions for expression of constructs, the
160 plants were subjected to the respective stress conditions.

161 **Protein extraction, SDS-PAGE, and Western blot**

162 Equal amounts of plant leaf tissue were ground in liquid nitrogen using metal beads. Total
163 proteins were extracted using a protein extraction buffer (50 mM Tris, pH 8; 20 mM NaCl;
164 10 % glycerol; 0.5 % Triton X-100; 1x Protease Inhibitor). Samples were mixed thoroughly,
165 incubated on ice for 10 min, and centrifuged (14 000 rpm, 10 min, 4 °C). The supernatant was
166 collected, mixed with SDS-PAGE sample buffer, and incubated at 80 °C for 5 min. Total
167 proteins were separated by SDS-PAGE and transferred to a polyvinylidene difluoride
168 membrane. Equal loading was validated using Coomassie Brilliant Blue staining of the
169 membrane before the remaining unspecific protein binding sites were blocked with blocking
170 solution (3 % milk + 2 % BSA in 1x PBST). For immunodetection, primary antibodies (anti-
171 GFP: Abcam ab290) from rabbit were used in combination with a secondary HRP-conjugated
172 anti-rabbit antibody from goat. For repeated detection of proteins from one membrane,
173 membranes were first dried and then re-wetted with 1x PBST before Coomassie Brilliant Blue
174 staining. The membranes were stripped by incubation in stripping buffer (200 mM glycine;
175 3.5 mM SDS; 1 % Tween 20; pH 2.2) for 20 min and subsequent washing with 1x PBST (3x
176 for 5 min). Membranes were re-blocked with blocking solution prior to re-probing with the new
177 antibody.

178 **GC-MS analysis**

179 Plant metabolites from *N. benthamiana* were extracted following an established protocol for
180 GC-MS-based metabolite profiling (Lisec et al., 2006), with minor modifications. In short, the

181 samples (25 mg leaf tissue per sample with six biological replicates per treatment) were
182 extracted in methanol containing an internal standard (Pentaerythritol, stock concentration
183 0.6 mg/ml in DDW, final concentration 0.016 mg/ml), shaken for 15 min at 70 °C, and
184 centrifuged at 14 000 rpm for 10 min. The supernatant was transferred to new tubes, and
185 chloroform and double-distilled water were added. The mixture was centrifuged at 14 000 rpm
186 for 15 min, and aliquots of 200 µL of the upper phase of each sample were transferred to new
187 tubes and dried by Speedvac, overnight. Derivatization was carried out as previously described
188 (Lisec et al., 2006). Polar metabolites were measured by the Agilent 7200B GC/Q-TOF. The
189 injection and separation procedures were performed according to Dahtt using the DB-35MS
190 column (Dhatt et al., 2019). Metabolite detection and annotation were performed by Quant
191 software (Agilent, Santa Clara, CA, USA), according to an accurate mass library of known
192 markers generated by our group and run in the same system. Following blank subtraction, the
193 peak area of each metabolite was normalized to the internal standard (i.e., Pentaerythritol) in
194 each sample, as well as to the fresh weight of the respective sample. For more information, see
195 Table S1.

196 **Statistical analysis and data visualization**

197 Data were statistically examined using analysis of variance (Ordinary one-way ANOVA) and
198 tested for significant differences using unpaired *t* tests using GraphPad Prism 8.0.1 software.
199 Graphs and were generated using GraphPad Prism 8.0.1, while Principal component analysis
200 (PCA) of the metabolome was performed using Metaboanalyst, an open-source, web-based tool
201 for metabolomics data analysis (https://www.metaboanalyst.ca/). Heatmaps were generated
202 using the MultiExperiment Viewer (MeV) freely available software application (Howe at al,
203 2010). Western blots were processed to maximize readers accessibility to the data. Original
204 blots can be found in the supplemental data (FigS3).
205

206 **<u>Results</u>**

207 **Heat stress facilitates bacterial growth in an autophagy-dependent manner**

208 Autophagy functions in plant biotic and abiotic stress response (Avin-Wittenberg, 2019,
209 Sertsuvalkul et al., 2022). Yet, very few studies investigated the role of autophagy in a combined
210 stress scenario, which is closer to the conditions faced by plants in the field. We chose to
211 examine two stresses in which autophagy was shown to play a role: heat stress and *Xcv* infection
212 (Leong et al., 2022b, Zhou et al., 2014). We began with assessing the growth of *Xcv* following
213 heat treatment of its natural host tomato (*Solanum lycopersicum*). Tomato M82 plants were

214 infiltrated with *Xcv* following 6h heat stress. Bacterial titers were checked 3 days post-infection
215 (dpi) (Fig1A). *Xcv* grew better in heat-stressed plants (Fig1B). Surprisingly, this beneficial
216 effect of preceding heat stress on bacterial growth was dependent on autophagy. In the presence
217 of the autophagy inhibitor 3-Methyadenine (3-MA), preceding heat stress did not affect
218 bacterial growth. Interestingly, pre-treatment with 3-MA without heat stress did not alter
219 bacterial growth. We thus postulated that activation of autophagy during heat stress facilitates
220 bacterial growth.
221 Over-expression of ATG7 was shown to increase autophagic activity in Arabidopsis (Minina et
222 al., 2018). Thus, we aimed to overexpress ATG7 and assess bacterial growth. To that end, we
223 switched to a *Nicotiana benthamiana* system, in which autophagy following *Xcv* infection has
224 been previously investigated and transient overexpression is easily performed (Leong et al.,
225 2022b). Although *N. benthamiana* is not a natural host of *Xcv*, the mutant line Δ*roq1* (Grutzner
226 et al., 2021) can be infected by the bacteria. We initially examined whether the phenomenon
227 observed in tomato also occurs in *N. benthamiana*. We infiltrated *Xcv* into *N. benthamiana*
228 Δ*roq1* plants after 6h heat stress. As in the tomato system, we observed increased bacterial
229 growth following heat stress, which was attenuated by autophagy inhibition (Fig1C). The
230 differences in the *N. benthamiana* system were even more pronounced than in tomato. We
231 observed a slight yet significant decrease in bacterial growth following 3-MA treatment under
232 control conditions (Fig1C). We thus wished to verify that the 3-MA treatment itself did not
233 affect bacterial growth. We incubated *Xcv* in an infiltration medium with and without 3-MA
234 and pated the bacteria directly to assess growth. There was no difference in bacterial titters
235 between treatments (control: log10cfu/cm^2 4.25±0.11, 3-MA: log10 cfu/cm^2 4.28±0.08, n=4,
236 no significant difference found in student's *t-test*). Next, we tested bacterial performance with
237 and without preceding heat stress in *N. benthamiana* plants transiently expressing *AtATG7*. As
238 expected, in plants transiently overexpressing *AtATG7*, *Xcv* grew similarly in heat-stressed and
239 unstressed plants (Fig1D), suggesting that autophagy activation, irrespective of its cause, is
240 conducive to bacterial growth.

241 **Different ATG8 homologs are involved in stress-related autophagy**

242 As we postulated that autophagy activation by heat stress before *Xcv* infection benefits bacterial
243 growth, we wished to determine that autophagy is indeed activated under these conditions. We
244 focused on ATG8, which is anchored to the autophagosome membrane. The GFP-ATG8 fusion
245 construct is used as a common autophagosome marker. Moreover, as ATG8 is degraded in the
246 vacuole, the ratio of GFP-ATG8 and free GFP resealed following degradation is used as a proxy

of autophagic flux (Klionsky et al., 2021). ATG8 exists as a gene family in plants and also functions in target recognition and cargo binding for selective autophagy. We speculated that ATG8 isoform specificity may vary between stresses, which is yet to be determined (Kellner et al., 2017). We thus examined the degradation patterns of GFP-fusion constructs of the potato (*Solanum tuberosum*) *St*ATG8 isoforms under single and combined stresses. As our chosen biotic stress is a tomato pathogen, potato isoforms were used to mimic the tomato response to *Xcv* infection.

GFP-tagged versions of all seven *St*ATG8 isoforms were transiently expressed in *N. benthamiana*. The plants were then subjected to heat stress, *Xcv* infection, and prolonged darkness. Prolonged darkness leads to carbon starvation, widely known to induce autophagy, presumably in a non-selective manner (Barros et al., 2017), and was therefore used as a positive control. Carbon starvation was induced by three days of darkness, leading to increased degradation of all GFP-*St*ATG8 isoforms and high levels of free GFP (Fig2A). Heat stress reduced protein levels of all GFP-*St*ATG8 isoforms after 6 h and 8 h of 40°C, yet we were not able to observe a free GFP band in all the samples, and thus compared Protein levels to the non-treated (control) plants (Fig2B). However, ATG8 degradation differed in timing and intensity. While some isoforms responded quickly (after 6 h), others showed a slower reduction upon stress (after 8 h). GFP-*St*ATG8-3.1 and GFP-*St*ATG8-4 showed a quick, strong, and lasting decrease in protein levels.

Next, we tested the effect of infection with *Xcv*. Only a subset of GFP-*St*ATG8 isoforms was degraded upon *Xcv* challenge (Fig2C). The GFP-*St*ATG8-2 isoforms, GFP-*St*ATG8-3.1, and in some but not all experimental replicates, GFP-*St*ATG8-4 displayed increased degradation upon *Xcv* infection. GFP-*St*ATG8-1 isoforms showed the opposite effect. Interestingly, the *Xcv*-specific activation of GFP-*St*ATG8 isoforms was independent of bacterial effectors. Infection with the T3SS mutant *Xcv* Δ*hrcV* (hereafter called *hrcV*), lacking the effector secretion system (Cerutti et al., 2017), resulted in a GFP-ATG8 degradation pattern similar to that of *Xcv*. Surprisingly, the detected degradation band was not free GFP, unlike the observed for carbon starvation. These results indicate a specific autophagic response to stress, particularly to *Xcv*/bacterial infection, unlike the non-specific reaction to general stressors like carbon starvation.

Differential autophagy activation under combined stress compared to single stresses

As *St*ATG8-3.1 was degraded upon heat stress as well as after inoculation with *Xcv*, we chose this isoform to assess autophagic activity in a combined heat-*Xcv* challenge. As performed in

280 the single-stress experiments, GFP-*St*ATG8-3.1 was transiently expressed in *N. benthamiana*
281 Δ*roq1* plants. The plants were then subjected to 6 h heat stress or 6 h *Xcv* infection. In addition,
282 6 h heat stress was followed by subsequent 6 h *Xcv* or a 6 h recovery period without *Xcv*
283 inoculation (Fig2D). Although *Xcv* inoculation was the second and, therefore, more recent
284 treatment, GFP-*St*ATG8-3.1 degradation after combined stress treatment resembled heat stress
285 instead of *Xcv* infection (Fig2E). Our results suggest that different ATG8 isoforms participate
286 in autophagy activation during different stresses and that stress combinations can further
287 influence autophagic flux in a non-additive manner. In the case of heat-*Xcv* challenge, preceding
288 heat indeed changed the nature of autophagy activation during infection, further strengthening
289 our hypothesis that pre-activation of autophagy promotes *Xcv* proliferation.

290 **Heat stress recovery fails to halt bacterial growth, but effector deficiency succeeds**

291 When we examined autophagy activation upon combined stresses, we also noticed that the
292 degradation pattern of GFP-ATG8 remained similar to heat stress after a 6h recovery period
293 (Fig2E). We thus wished to assess whether the phenomenon of increased bacterial growth
294 following heat stress also persisted after recovery. We, therefore, repeated bacterial growth
295 experiments with heat-stressed plants and prolonged the recovery period to 24 h (Fig3A).
296 Comparable to results without a recovery period, previous heat treatment resulted in increased
297 bacterial growth even after the recovery period (unpaired *t-test* p-value 0.0067), although not
298 significantly different in the ANOVA (Fig3B). As seen without the recovery period, this effect
299 was again autophagy-dependent. These results suggest that autophagy induction upon heat
300 stress has a lasting effect on the internal plant environment, impacting bacterial growth.
301 Our Western blot analyses also revealed that autophagy activation by *Xcv* is effector-
302 independent (Fig2C). Thus, we wished to examine whether effectors play a role in autophagy-
303 mediated bacterial growth and examined the *hrcV* mutant following heat stress. Interestingly,
304 the mutant did not benefit from previous heat stress in the host plants (Fig3C), and autophagy
305 inhibition by 3-MA did not affect its growth either. We thus postulate that although autophagy
306 is activated by bacterial infection in an effector-independent manner, the autophagy-dependent
307 increase in bacterial growth after heat stress is also dependent on bacterial effector delivery.

308 **Metabolic shift caused by *Xcv* is treatment-resilient**

309 Recognizing autophagy's role in plant nutrient availability (Signorelli et al., 2019), we theorized
310 that its activation during heat stress might reshape metabolic content to favor bacterial growth.
311 We performed metabolic profiling via Gas Chromatography-Mass Spectrometry (GC-MS) on
312 previously heat-stressed *N. benthamiana* leaf tissue infected with bacteria (Fig4A). We

concentrated on primary metabolites, representing nutrients potentially utilized by the bacteria. Principal component analysis (PCA) showed a major shift between non-treated plants (red) and samples from heat-treated plants (yellow) (Fig4B). *Xcv*-inoculation led to another shift. All samples that received *Xcv*-treatment clustered together independent of additional treatments. Samples from *hrcV*-infected plants were also analyzed to assess the influence of effectors on metabolism. Most of the *hrcV*-treated samples clustered with the *Xcv*-treated samples, yet some clustered away from the *Xcv*-treated samples in the PCA, pointing to a slight effector-dependent shift of the metabolome (Fig4B). We also included samples in which plants had a 24 h recovery period from heat before infection. In accordance with the bacterial growth assay, the recovery period did not affect the metabolic profile of the samples (FigS1).

Generally, heat-treated plants as well as *Xcv*-infected plants, showed strong differences from control plants in most identified compounds (Fig4C). Many of the metabolites were depleted. In particular, sugars and amino acids were reduced under heat stress and after infection, respectively. In contrast, the sugar alcohol Myo-inositol increased, specifically after heat challenge (see below). Collectively, our findings indicate stress-induced metabolic shifts, with stress-specific patterns yet common alterations in energy sources. Notably, the response to *Xcv* infection exhibited remarkable resilience to additional factors or stresses.

Changes in organic acids are independent of autophagy

We next focused on specific metabolic changes induced by stress combinations and their dependence on autophagy. No changes in shikimic acid levels were detected in response to heat stress, but levels were reduced significantly in response to infection or a combined heat-pathogen stress (FigS2A). This response to infection was independent of autophagy and similar in *Xcv* and *hrcV*. Nicotinic acid showed a mild reduction under combined stress compared to the single stresses, which was significantly lower than in control plants (FigS2B). Again, the response to combined stress was independent of autophagy. Two compounds of the TCA cycle, succinic acid and malic acid, were reduced only upon heat treatment but not infection (FigS2E,F). However, while levels of malic acid stayed low in all plants that previously received heat treatment, *Xcv* but not *hrcV* infection restored control levels of succinic acid in heat-stressed plants in an autophagy-independent manner. The levels of a third detected member of the TCA cycle, citric acid, did not change in response to any stress treatment (FigS2G). Together, our results suggest that changes in organic acids in response to stress combinations are not dependent on autophagy.

Shift in amino acid levels is independent of bacterial effectors

346 We directed our attention to metabolites functioning as energy sources. Amino acids are a major
347 energy source that can be mobilized under stress (Signorelli et al., 2019). We detected three
348 amino acids, which were generally reduced upon bacterial infection as well as heat stress,
349 especially in the case of glycine (Fig5A,B). *Xcv* and *hrcV* showed a similar effect. Asparagine
350 was reduced upon bacterial infection and further reduced in the presence of 3-MA under control
351 conditions (Fig6C). This effect was also observed in heat-stressed plants but to a lesser extent.
352 Thus, the shifts in amino acid levels are not a result of bacterial manipulation but rather a
353 general response of the plant to stress conditions. Urea levels, a metabolite directly linked to
354 amino acid catabolism (Witte, 2011), stayed stable upon heat challenge but were reduced upon
355 *Xcv* infection, independent of temperature (Fig6D). Interestingly, *hrcV* treatment significantly
356 increased urea levels in an autophagy-dependent and heat-sensitive manner.

357 **Effector-dependent reduction of sugars is heat-sensitive and modulated by autophagy**

358 Sugars are a main energy source under stress conditions (Signorelli et al., 2019). Most of the
359 mono- and disaccharides were globally decreasing upon heat- and *Xcv*-treatment compared to
360 control samples, with sucrose showing only a decrease upon infection, not heat (Fig7A-C, E-
361 G). This effect was not influenced by 3-MA treatment. Samples treated with *hrcV* displayed a
362 more minor sugar reduction than *Xcv* infection (significant only for Glucose). However, when
363 autophagy was inhibited by 3-MA treatment, *hrcV* infection reduced sugar levels to a similar
364 extent as after *Xcv* infection. The effect of *Xcv* treatment was not further intensified by 3-MA
365 treatment, as seen for *hrcV*. We, therefore, suggest that the decrease in sugar levels upon
366 infection is partially dependent on effector(s) targeting autophagy. Interestingly, the effect
367 observed for *hrcV* was only present in control conditions and absent in heat-stressed plants
368 where *Xcv* and *hrcV* infection had similar, autophagy-independent effects.
369 The only detected Monosaccharide that did not fit into the described pattern is Xylose/Lyxose
370 (Fig7D). Levels of this sugar were not reduced upon *Xcv* infection or heat treatment but only
371 upon inhibition of autophagy, pointing to a role of autophagy in maintaining Xylose/Lyxose
372 levels under stress conditions.
373 Myo-inositol did not change upon *Xcv* infection (Fig7H). However, levels increased
374 significantly upon *hrcV*-treatment in an autophagy-dependent manner. Heat stress led to a
375 general increase in Myo-inositol levels, a well-documented response to heat and other abiotic
376 stresses in different plant species (Khurana et al., 2017, Sharma et al., 2020, Boominathan et
377 al., 2004). Combined heat-*Xcv* but not heat-*hrcV* stress reduced these levels significantly in an
378 autophagy-dependent manner (ANOVA performed in the absence of control *hrcV* samples). The

massive shifting of sugars is, at least partially, the result of an effector-mediated, heat-sensitive inhibition of autophagy by *Xcv*. Taken together, our detailed metabolic profiling showed a strong effect of the applied stress (combinations) on metabolites mainly involved in primary (energy) metabolism. For most sugars and urea, the impact of *Xcv* infection was effector-dependent and absent in *hrcV*. This effector-dependent effect was mimicked in *hrcV* by inhibition of autophagy.

Discussion

The simultaneous occurrence of environmental stresses, such as heat, with pathogen infection poses a widespread threat to plant health. Understanding how plants navigate these dual challenges is crucial to enhancing crop breeding initiatives and creating robust varieties. In this study, we highlight autophagy as a fundamental mechanism that bestows stress-specific capabilities upon plants.

Response to combined abiotic-biotic stress is very complex, involving the interaction of two living organisms (the plant and the pathogen) as well as the additional level of abiotic stress (Kissoudis et al., 2014). Subjecting the plants to heat while concurrently exposing them to *Xcv* implies that both the plants and the bacteria are experiencing above-optimum temperatures. We tried to reduce the level of complexity by applying the combined heat-*Xcv* stress as a consecutive stress where the bacteria are not experiencing direct heat stress. Studies investigating combined stresses usually focus on a single time point; however, we believe that our experimental system of a consecutive stress setup reflects a natural situation more accurately where stress may also occur sequentially rather than simultaneously.

Active autophagy in the host before infection facilitates bacterial growth

We observed that *Xcv* growth after infection was enhanced by preceding heat stress in the pathogen's native host, tomato, as well as the model plant *N. benthamiana*, in an autophagy-dependent manner (Fig1A,B). Enhanced growth of another bacterial phytopathogen, *Pseudomonas Pst* DC300, at moderately elevated temperature during infection has been described before (Huot et al., 2017). As in our case, the increased growth depended on the delivery of bacterial effector proteins (Fig3C). We can now link this enhanced growth to bacterial manipulation of autophagy. Interestingly, over-expression of *ATG7* prior to infection yielded similar results, suggesting that other abiotic stresses inducing autophagy (such as drought or salt stress; (Avin-Wittenberg, 2019)) might elicit similar susceptibility to bacterial infection.

412 The specific effector utilizing the pre-activation of autophagy by heat to facilitate bacterial
413 growth is still unknown. So far, one *Xcv* effector, XopL, has been shown to regulate autophagy.
414 Yet, it inhibits autophagy rather than utilizing it (Leong et al., 2022b). Our findings highlight
415 the debate regarding the dual role of autophagy in pathogen resistance, promoting or inhibiting
416 pathogen growth in a context-dependent manner (Mostowy, 2013). One possibility is that an
417 effector other than XopL utilizes autophagy pre-activation to promote growth, which could not
418 be identified in conditions where autophagy is not pre-activated. Another possibility is that the
419 role of autophagy in immunity is indeed context-dependent, i.e., the autophagic response
420 integrates several signals to produce a specific output.

421 **ATG8 confers specificity to combined plant stress responses**

422 Autophagy can selectively remove damaged or unwanted cellular components. The selectivity
423 is conferred by target binding to autophagy receptors, which, in turn, bind ATG8 (Stephani and
424 Dagdas, 2020). Thus, although many conditions induce autophagy, the autophagic cargo and
425 the resulting degradome are expected to be unique to each condition. Since plants have multiple
426 ATG8 isoforms, it has been proposed that these isoforms play a crucial role in shaping the
427 stress-specific response and selectivity of autophagy (Kellner et al., 2017, Lin et al., 2023, Zess
428 et al., 2019). There are two main methods to study autophagy activation using GFP-ATG8. The
429 GFP tag enables autophagosome visualization by confocal microscopy. In addition, the ratio
430 between GFP-ATG8 and free GFP by Western blot allows us to estimate ongoing autophagic
431 flux (Klionsky et al., 2021). We could not detect free GFP in our *N. benthamiana* Western blots,
432 apart from plants exposed to dark conditions (Fig2A-C). In fact, we often and repeatedly only
433 detected an unknown but GFP-specific degradation band. Similar bands were reported in other
434 plant species (Zhou et al., 2023), yet their existence was not explained. This novel band is
435 clearly connected to the degradation of GFP-*St*ATG8, and is absent without GFP-*St*ATG8
436 protein. Therefore, we decided to use this degradation band instead of free GFP to calculate the
437 ratio between its intensity and GFP-*St*ATG8.

438 In our study, the seven *St*ATG8 isoforms exhibited stress-specific responses based on the type
439 of stress (Fig2A-C). Carbon starvation triggered a uniform degradation of all isoforms, whereas
440 *Xcv* infection or heat differed in ATG8 activation pattern. Bacterial infection is hampered by
441 removing effector proteins via autophagy (Leong et al., 2022b). Accordingly, only selected
442 *St*ATG8 isoforms were activated by *Xcv* infection. By contrast, under heat stress, *St*ATG8
443 isoforms differed in degradation timing. Heat stress generally causes protein aggregation, but
444 proteins vary in their ability to withstand elevated temperatures. We suggest *St*ATG8 isoforms
445 are degraded at different times during heat stress to account for the variability in protein heat

sensitivity and, thus, their need for clearance. One of the unique structural features of ATG8 proteins is an N-terminal helix domain (Bu et al., 2020). This domain determines the binding specificity to ATG8-interacting proteins, and its sequence is not conserved in plants (Zess et al., 2019). Thus, preferential binding of ATG8 isoforms to different targets and selective autophagy receptors seems only logical (Kellner et al., 2017). Besides differential activation of ATG8 proteins, expression of *AtATG8* genes differed when exposed to starvation or (a)biotic stress (Wang et al., 2019, Chiu et al., 2023, Leong et al., 2022b), further confirming our finding of stress-specific involvement of *St*ATG8 isoforms.

GFP-*St*ATG8-3.1 was involved in the response to heat stress and *Xcv* infection (Fig2B,C). Yet, when exposed to a combined heat-*Xcv* challenge, the activation did not mimic a combination of both stresses (Fig2E). Hence, the assumption that combined stresses equal the sum of the involved single stresses falls short of the complexity of natural systems. There is a possibility that combined stress activates another suite of *St*ATG8 isoforms than the single stresses. The Western blot results strengthen our infection assays with *Xcv*, suggesting that the autophagic response is tailored to integrate several stresses.

Changes in metabolites as an underestimated effect of autophagy influencing bacterial performance

Nutrient availability plays a major role in pathogen growth. We thus asked whether previous heat stress affected nutrient availability for the invading pathogen. Due to technical constraints, our metabolic profiling focused on a sinlge time point, missing the dynamic regulation of metabolism. In addition, the large variation and lack of significant differences were disappointing. The experiment involved ten treatments and six biological replicates per treatment. The procedure was carefully controlled, including chamber transfers for temperature treatment and manual syringe infiltration for *Xcv* and *hrcV* treatments. However, potential changes in light quality and humidity between the experimental chamber and the cultivation room might have influenced metabolite levels. Additionally, the time-consuming tasks of harvesting two leaves per plant made precise 1-hour (60 min) sample collection impractical, resulting in a more realistic time range of 55 to 75 mins. However, we could come to several conclusions linking autophagy, bacterial effectors, and plant metabolism.

Nutrients in the apoplast available for bacterial nutrition are mainly sugars and amino acids (Rico and Preston, 2008, Fatima and Senthil-Kumar, 2015). Sugars and amino acids were generally reduced in the tested leaf tissue as a result of heat stress and also after infection. This observation is not surprising, given that stress responses are energetically costly (Signorelli et

al., 2019). While we saw this reduction in amino acids upon *Xcv* infection (Fig4C), we cannot confirm it results from bacterial manipulation of autophagy or bacterial consumption of these metabolites. Urea, linked to amino acid catabolism (Witte, 2011), displayed an opposite response to stress. While amino acid levels decreased upon infection, heat stress alone had no major effect on urea levels, and *Xcv* infection or combined stress even slightly reduced urea levels (Fig5D). Interestingly, this reduction resulted from bacterial manipulation as levels increased significantly following *hrcV* infection. More importantly, this increase was absent when *hrcV* infection was combined with autophagy inhibition. Amino acids are recycled from proteins degraded via autophagy.

In addition, components targeted by bacterial effectors to manipulate metabolite recycling via autophagy might be heat-sensitive. When *hrcV* infection followed heat stress, urea levels were reduced, resembling *Xcv* infection. The absence of increased urea in combined *hrcV*-heat stress can also be explained on a more general immune response level. Salicylic acid (SA) is the dominant phytohormone involved in the plant's defense against (hemi)biotrophic pathogens. This SA response is heat sensitive in Arabidopsis and tobacco (Wang et al., 2009). Loss of pathogen-induced SA was described as a central mechanism underlying enhanced bacterial growth of *Pseudomonas Pst* DC300 at elevated temperatures (Huot et al., 2017). Without an energy-intensive immune response, amino acids would not be channeled into energy production, failing to increase urea levels.

Xcv infection at least partially manipulates sugar levels in an autophagy-dependent manner, which seems to be mimicked by heat stress (Fig6). During infection, phytopathogens can adjust their metabolic machinery towards the most abundant nutrients in the host. *Xcv* was shown to modulate its manner of active nutrient acquisition (Fatima and Senthil-Kumar, 2015). So-called TBDTs (TonB-dependent transporters) are involved in uptake of carbohydrates, with genomes of several *Xanthomonas* species having a high copy number of TBDT genes (Blanvillain et al., 2007, Dugé de Bernonville et al., 2014, Pieretti et al., 2012). Moreover, pathogens like *Xcv*, colonizing the apoplast, release effector proteins to manipulate plant cells and optimize nutrient availability, e.g. by facilitating sugar efflux through induction of gene expression of sugar transporters (Chen et al., 2010, Eom et al., 2015, Zhou et al., 2015).

In addition to effectors influencing nutrient efflux, pathogens target autophagy directly (Üstün et al., 2016, Lal et al., 2020, Leong et al., 2022a). The reduction of sugar levels is partially dependent on effector proteins, as the *hrcV* mutant was unable to reduce sugar levels comparable to *Xcv*. Inhibition of autophagy by 3-MA led to *Xcv*-like sugar levels after *hrcV* infection, suggesting that the reduced sugar levels after Xcv infection resulted from autophagy

inhibition by bacterial effectors. The autophagy-dependent manipulation of sugar levels is no longer observable when *hrcV* infection follows heat stress. Since heat stress affects autophagic activity (Zhou et al., 2014) and thereby also metabolite recycling, manipulation of autophagy might be obsolete under these conditions. Another interpretation is that, as mentioned above, the effector targets are heat sensitive, and this manipulation is no longer needed when the infection follows a heat stress. However, the effect of *Xcv* on sugar levels does not solely depend on autophagy, as autophagy inhibition by 3-MA did not alter the *Xcv* sugar phenotype. We thus postulate that manipulation of autophagy is not the only mechanism underlying pathogen success. This observation also explains why *Xcv* growth benefits from preceding heat stress whereas *hrcV* growth does not (Fig1B,C&3C). While the *hrcV* sugar phenotype can be compensated by preceding heat stress, the *hrcV* growth phenotype is unaffected, presumably because there are other effectors contributing to pathogen success than those targeting autophagy. As *hrcV* can not secrete any effectors to the plant, future studies using more specific effector mutants might be able to discern the particular effects of bacterial effectors in autophagy-dependent nutrient availability.

Our findings underscore the specificity inherent in the autophagic response, particularly regarding ATG8 isoforms. We demonstrate that combined stresses do not equal the sum of their counterparts, specifically focusing on autophagy at the nexus of simultaneous challenges. It will be interesting to see if the specificity of the autophagic response, especially in the case of stress combinations, also translates to the autophagic cargo level. The influence of heat stress on autophagy, seen in its facilitation of bacterial growth, establishes it as a key link between environmental factors and plant-microbial interactions. This connection underscores the broader ecological implications of autophagy in plant defense and unveils potential targets for enhancing stress resilience. As autophagy functions in many aspects of plant life, it is not possible to distinguish its roles in nutrient supply, abiotic stress, and pathogen defense. As our results show, it is possible that other, still unknown factors contribute to autophagy-dependent bacterial growth following heat stress.

Acknowledgments

We thank the Rachel Green and Omri Finkel groups at HUJI for assistance with heatable phytochambers and Elena Minina, Johannes Stuttmann, Yasin Dagdas, and Guido Sessa for sharing transgenic seeds, bacterial strains and plasmids. Fig. 1A, 2D, 3A and 4A were created with Biorender (https://www.biorender.com). The project was funded by a Walter-Benjamin Fellowship to HS by Deutsche Forschungsgemeinschaft (Projektnummer 446674370).

Author Contributions

HS and TAW designed the research; HS, EK, YS and TAW performed research experiments; HS, YS and TAW analyzed data; HS and TAW wrote the manuscript with input from all authors.

References

ATKINSON, N. J. & URWIN, P. E. 2012. The interaction of plant biotic and abiotic stresses: from genes to the field. *Journal of Experimental Botany,* 63**,** 3523-3543.

AVIN-WITTENBERG, T. 2019. Autophagy and its role in plant abiotic stress management. *Plant, Cell & Environment,* 42**,** 1045-1053.

BARROS, J. A. S., CAVALCANTI, J. H. F., MEDEIROS, D. B., NUNES-NESI, A., AVIN-WITTENBERG, T., FERNIE, A. R. & ARAÚJO, W. L. 2017. Autophagy Deficiency Compromises Alternative Pathways of Respiration following Energy Deprivation in Arabidopsis thaliana. *Plant Physiology,* 175**,** 62-76.

BAXTER, A., MITTLER, R. & SUZUKI, N. 2013. ROS as key players in plant stress signalling. *Journal of Experimental Botany,* 65**,** 1229-1240.

BEBBER, D. P. 2015. Range-Expanding Pests and Pathogens in a Warming World. *Annual Review of Phytopathology,* 53**,** 335-356.

BLANVILLAIN, S., MEYER, D., BOULANGER, A., LAUTIER, M., GUYNET, C., DENANCÉ, N., VASSE, J., LAUBER, E. & ARLAT, M. 2007. Plant Carbohydrate Scavenging through TonB-Dependent Receptors: A Feature Shared by Phytopathogenic and Aquatic Bacteria. *PLoS ONE,* 2.

BOOMINATHAN, P., SHUKLA, R., KUMAR, A., MANNA, D., NEGI, D., VERMA, P. K. & CHATTOPADHYAY, D. 2004. Long Term Transcript Accumulation during the Development of Dehydration Adaptation in Cicer arietinum *Plant Physiology,* 135**,** 1608-1620.

BU, F., YANG, M., GUO, X., HUANG, W. & CHEN, L. 2020. Multiple Functions of ATG8 Family Proteins in Plant Autophagy. *Frontiers in Cell and Developmental Biology,* 8.

CAVICCHIOLI, R., RIPPLE, W. J., TIMMIS, K. N., AZAM, F., BAKKEN, L. R., BAYLIS, M., BEHRENFELD, M. J., BOETIUS, A., BOYD, P. W., CLASSEN, A. T., CROWTHER, T. W., DANOVARO, R., FOREMAN, C. M., HUISMAN, J., HUTCHINS, D. A., JANSSON, J. K., KARL, D. M., KOSKELLA, B., MARK WELCH, D. B., MARTINY, J. B. H., MORAN, M. A., ORPHAN, V. J., REAY, D. S., REMAIS, J. V., RICH, V. I., SINGH, B. K., STEIN, L. Y., STEWART, F. J., SULLIVAN, M. B., VAN OPPEN, M. J. H., WEAVER, S. C., WEBB, E. A. & WEBSTER, N. S. 2019. Scientists' warning to humanity: microorganisms and climate change. *Nature Reviews Microbiology,* 17**,** 569-586.

CERUTTI, A., JAUNEAU, A., AURIAC, M. C., LAUBER, E., MARTINEZ, Y., CHIARENZA, S., LEONHARDT, N., BERTHOME, R. & NOEL, L. D. 2017. Immunity at Cauliflower Hydathodes Controls Systemic Infection by Xanthomonas campestris pv campestris. *Plant Physiol,* 174**,** 700-716.

CHEN, L.-Q., HOU, B.-H., LALONDE, S., TAKANAGA, H., HARTUNG, M. L., QU, X.-Q., GUO, W.-J., KIM, J.-G., UNDERWOOD, W., CHAUDHURI, B., CHERMAK, D., ANTONY, G., WHITE, F. F., SOMERVILLE, S. C., MUDGETT, M. B. & FROMMER, W. B. 2010. Sugar transporters for intercellular exchange and nutrition of pathogens. *Nature,* 468**,** 527-532.

CHEN, Y. & KLIONSKY, D. J. 2011. The regulation of autophagy – unanswered questions. *Journal of Cell Science,* 124**,** 161-170.

CHIU, C.-Y., LUNG, H.-F., CHOU, W.-C., LIN, L.-Y., CHOW, H.-X., KUO, Y.-H., CHIEN, P.-S., CHIOU, T.-J. & LIU, T.-Y. 2023. Autophagy-Mediated Phosphate Homeostasis in Arabidopsis Involves Modulation of Phosphate Transporters. *Plant And Cell Physiology,* 64**,** 519-535.

CHUNG, T. 2019. How phosphoinositides shape autophagy in plant cells. *Plant Science,* 281**,** 146-158.

DAGDAS, Y. F., BELHAJ, K., MAQBOOL, A., CHAPARRO-GARCIA, A., PANDEY, P., PETRE, B., TABASSUM, N., CRUZ-MIRELES, N., HUGHES, R. K., SKLENAR, J., WIN, J., MENKE, F., FINDLAY, K., BANFIELD, M. J., KAMOUN, S. & BOZKURT, T. O. 2016. An effector of the Irish potato famine pathogen antagonizes a host autophagy cargo receptor. *Elife,* 5.

DAGDAS, Y. F., PANDEY, P., TUMTAS, Y., SANGUANKIATTICHAI, N., BELHAJ, K., DUGGAN, C., LEARY, A. Y., SEGRETIN, M. E., CONTRERAS, M. P., SAVAGE, Z., KHANDARE, V. S., KAMOUN, S. & BOZKURT, T. O. 2018. Host autophagy machinery is diverted to the pathogen interface to mediate focal defense responses against the Irish potato famine pathogen. *Elife,* 7.

DHATT, B. K., ABSHIRE, N., PAUL, P., HASANTHIKA, K., SANDHU, J., ZHANG, Q., OBATA, T. & WALIA, H. 2019. Metabolic Dynamics of Developing Rice Seeds Under High Night-Time Temperature Stress. *Front Plant Sci,* 10**,** 1443.

DODDS, P. N. & RATHJEN, J. P. 2010. Plant immunity: towards an integrated view of plant–pathogen interactions. *Nature Reviews Genetics,* 11**,** 539-548.

DUGÉ DE BERNONVILLE, T., NOËL, L. D., SANCRISTOBAL, M., DANOUN, S., BECKER, A., SOREAU, P., ARLAT, M. & LAUBER, E. 2014. Transcriptional reprogramming and phenotypical changes associated with growth ofXanthomonas campestrispv.campestrisin cabbage xylem sap. *FEMS Microbiology Ecology,* 89**,** 527-541.

EOM, J.-S., CHEN, L.-Q., SOSSO, D., JULIUS, B. T., LIN, I. W., QU, X.-Q., BRAUN, D. M. & FROMMER, W. B. 2015. SWEETs, transporters for intracellular and intercellular sugar translocation. *Current Opinion in Plant Biology,* 25**,** 53-62.

FATIMA, U. & SENTHIL-KUMAR, M. 2015. Plant and pathogen nutrient acquisition strategies. *Frontiers in Plant Science,* 6.

FENG, Y., HE, D., YAO, Z. & KLIONSKY, D. J. 2013. The machinery of macroautophagy. *Cell Research,* 24**,** 24-41.

FRAIRE-VELAZQUEZ, S., RODRIGUEZ-GUERRA, R. & SANCHEZ-CALDERO, L. 2011. Abiotic and Biotic Stress Response Crosstalk in Plants. *Abiotic Stress Response in Plants - Physiological, Biochemical and Genetic Perspectives.*

GLAZEBROOK, J. 2005. Contrasting Mechanisms of Defense Against Biotrophic and Necrotrophic Pathogens. *Annual Review of Phytopathology,* 43**,** 205-227.

GRUTZNER, R., MARTIN, P., HORN, C., MORTENSEN, S., CRAM, E. J., LEE-PARSONS, C. W. T., STUTTMANN, J. & MARILLONNET, S. 2021. High-efficiency genome editing in plants mediated by a Cas9 gene containing multiple introns. *Plant Commun,* 2**,** 100135.

HAFREN, A., MACIA, J. L., LOVE, A. J., MILNER, J. J., DRUCKER, M. & HOFIUS, D. 2017. Selective autophagy limits cauliflower mosaic virus infection by NBR1-mediated targeting of viral capsid protein and particles. *Proc Natl Acad Sci U S A,* 114**,** E2026-E2035.

HAFREN, A., USTUN, S., HOCHMUTH, A., SVENNING, S., JOHANSEN, T. & HOFIUS, D. 2018. Turnip Mosaic Virus Counteracts Selective Autophagy of the Viral Silencing Suppressor HCpro. *Plant Physiol,* 176**,** 649-662.

HEY, S. J., BYRNE, E. & HALFORD, N. G. 2009. The interface between metabolic and stress signalling. *Annals of Botany,* 105**,** 197-203.

HOWE E., HOLTON K., NAIR S., SCHLAUCH D., SINHA R., QUACKENBUSH J. 2010. MeV: MultiExperiment Viewer. *Biomedical Informatics for Cancer Research*, 267-277.

HUOT, B., CASTROVERDE, C. D. M., VELÁSQUEZ, A. C., HUBBARD, E., PULMAN, J. A., YAO, J., CHILDS, K. L., TSUDA, K., MONTGOMERY, B. L. & HE, S. Y. 2017. Dual impact of elevated temperature on plant defence and bacterial virulence in Arabidopsis. *Nature Communications,* 8.

ISLAM, M. R., FENG, B., CHEN, T., TAO, L. & FU, G. 2018. Role of Abscisic Acid in Thermal Acclimation of Plants. *Journal of Plant Biology,* 61**,** 255-264.

JONES, J. D. G. & DANGL, J. L. 2006. The plant immune system. *Nature,* 444**,** 323-329.

KELLNER, R., DE LA CONCEPCION, J. C., MAQBOOL, A., KAMOUN, S. & DAGDAS, Y. F. 2017. ATG8 Expansion: A Driver of Selective Autophagy Diversification? *Trends Plant Sci,* 22**,** 204-214.

KHURANA, N., SHARMA, N. & KHURANA, P. 2017. Overexpression of a heat stress inducible, wheat myo-inositol-1-phosphate synthase 2 (TaMIPS2) confers tolerance to various abiotic stresses in Arabidopsis thaliana. *Agri Gene,* 6**,** 24-30.

KISSOUDIS, C., VAN DE WIEL, C., VISSER, R. G. F. & VAN DER LINDEN, G. 2014. Enhancing crop resilience to combined abiotic and biotic stress through the dissection of physiological and molecular crosstalk. *Frontiers in Plant Science,* 5.

KLIONSKY, D. J., ABDEL-AZIZ, A. K., ABDELFATAH, S., ABDELLATIF, M., ABDOLI, A., ABEL, S., ABELIOVICH, H., ABILDGAARD, M. H., ABUDU, Y. P., ACEVEDO-AROZENA, A., ADAMOPOULOS, I. E., ADELI, K., ADOLPH, T. E., ADORNETTO, A., AFLAKI, E., AGAM, G., AGARWAL, A., AGGARWAL, B. B., AGNELLO, M., AGOSTINIS, P., AGREWALA, J. N., AGROTIS, A., AGUILAR, P. V., AHMAD, S. T., AHMED, Z. M., AHUMADA-CASTRO, U., AITS, S., AIZAWA, S., AKKOC, Y., AKOUMIANAKI, T., AKPINAR, H. A., AL-ABD, A. M., AL-AKRA, L., AL-GHARAIBEH, A., ALAOUI-JAMALI, M. A., ALBERTI, S., ALCOCER-GÓMEZ, E., ALESSANDRI, C., ALI, M., ALIM AL-BARI, M. A., ALIWAINI, S., ALIZADEH, J., ALMACELLAS, E., ALMASAN, A., ALONSO, A., ALONSO, G. D., ALTAN-BONNET, N., ALTIERI, D. C., ÁLVAREZ, É. M. C., ALVES, S., ALVES DA COSTA, C., ALZAHARNA, M. M., AMADIO, M., AMANTINI, C., AMARAL, C., AMBROSIO, S., AMER, A. O., AMMANATHAN, V., AN, Z., ANDERSEN, S. U., ANDRABI, S. A., ANDRADE-SILVA, M., ANDRES, A. M., ANGELINI, S., ANN, D., ANOZIE, U. C., ANSARI, M. Y., ANTAS, P., ANTEBI, A., ANTÓN, Z., ANWAR, T., APETOH, L., APOSTOLOVA, N., ARAKI, T., ARAKI, Y., ARASAKI, K., ARAÚJO, W. L., ARAYA, J., ARDEN, C., ARÉVALO, M.-A., ARGUELLES, S., ARIAS, E., ARIKKATH, J., ARIMOTO, H., ARIOSA, A. R., ARMSTRONG-JAMES, D., ARNAUNÉ-PELLOQUIN, L., AROCA, A., ARROYO, D. S., ARSOV, I., ARTERO, R., ASARO, D. M. L., ASCHNER, M., ASHRAFIZADEH, M., ASHUR-FABIAN, O., ATANASOV, A. G., AU, A. K., AUBERGER, P., AUNER, H. W., AURELIAN, L., et al. 2021. Guidelines for the use and interpretation of assays for monitoring autophagy (4th edition). *Autophagy***,** 1-382.

LAI, Z., WANG, F., ZHENG, Z., FAN, B. & CHEN, Z. 2011. A critical role of autophagy in plant resistance to necrotrophic fungal pathogens. *Plant J,* 66**,** 953-68.

LAL, N. K., THANASUWAT, B., HUANG, P.-J., CAVANAUGH, K. A., CARTER, A., MICHELMORE, R. W. & DINESH-KUMAR, S. P. 2020. Phytopathogen Effectors Use Multiple Mechanisms to Manipulate Plant Autophagy. *Cell Host & Microbe,* 28**,** 558-571.e6.

LENZ, H. D., HALLER, E., MELZER, E., KOBER, K., WURSTER, K., STAHL, M., BASSHAM, D. C., VIERSTRA, R. D., PARKER, J. E., BAUTOR, J., MOLINA, A., ESCUDERO, V., SHINDO, T., VAN DER HOORN, R. A., GUST, A. A. & NURNBERGER, T. 2011. Autophagy differentially controls plant basal immunity to biotrophic and necrotrophic pathogens. *Plant J,* 66**,** 818-30.

LEONG, JIA X., LANGIN, G. & ÜSTÜN, S. 2022a. Selective autophagy: adding precision in plant immunity. *Essays in Biochemistry,* 66**,** 189-206.

LEONG, J. X., RAFFEINER, M., SPINTI, D., LANGIN, G., FRANZ-WACHTEL, M., GUZMAN, A. R., KIM, J. G., PANDEY, P., MININA, A. E., MACEK, B., HAFREN, A., BOZKURT, T. O., MUDGETT, M. B., BORNKE, F., HOFIUS, D. & USTUN, S. 2022b. A bacterial effector counteracts host autophagy by promoting degradation of an autophagy component. *EMBO J,* 41**,** e110352.

LIN, L.-Y., CHOW, H.-X., CHEN, C.-H., MITSUDA, N., CHOU, W.-C. & LIU, T.-Y. 2023. Role of autophagy-related proteins ATG8f and ATG8h in the maintenance of autophagic activity in Arabidopsis roots under phosphate starvation. *Frontiers in Plant Science,* 14.

LIPPOK, B., BIRKENBIHL, R. P., RIVORY, G., BRÜMMER, J., SCHMELZER, E., LOGEMANN, E. & SOMSSICH, I. E. 2007. Expression of AtWRKY33 Encoding a Pathogen- or PAMP-Responsive WRKY Transcription Factor Is Regulated by a Composite DNA Motif Containing W Box Elements. *Molecular Plant-Microbe Interactions®,* 20**,** 420-429.

LISEC, J., SCHAUER, N., KOPKA, J., WILLMITZER, L. & FERNIE, A. R. 2006. Gas chromatography mass spectrometry-based metabolite profiling in plants. *Nat Protoc,* 1**,** 387-96.

LIU, Y. & BASSHAM, D. C. 2012. Autophagy: pathways for self-eating in plant cells. *Annu Rev Plant Biol,* 63**,** 215-37.

LUCK, J., SPACKMAN, M., FREEMAN, A., TRE˛BICKI, P., GRIFFITHS, W., FINLAY, K. & CHAKRABORTY, S. 2011. Climate change and diseases of food crops. *Plant Pathology,* 60**,** 113-121.

MAGEN, S., SEYBOLD, H., LALOUM, D. & AVIN-WITTENBERG, T. 2022. Metabolism and autophagy in plants—a perfect match. *FEBS Letters,* 596**,** 2133-2151.

MAO, G., MENG, X., LIU, Y., ZHENG, Z., CHEN, Z. & ZHANG, S. 2011. Phosphorylation of a WRKY Transcription Factor by Two Pathogen-Responsive MAPKs Drives Phytoalexin Biosynthesis in Arabidopsis *The Plant Cell,* 23**,** 1639-1653.

MARSHALL, R. S. & VIERSTRA, R. D. 2018. Autophagy: The Master of Bulk and Selective Recycling. *Annual Review of Plant Biology,* 69**,** 173-208.

MASCLAUX-DAUBRESSE, C., D'ANDREA, S., BOUCHEZ, I. & CACAS, J.-L. 2020. Reserve lipids and plant autophagy. *Journal of Experimental Botany,* 71**,** 2854-2861.

MININA, E. A., MOSCHOU, P. N., VETUKURI, R. R., SANCHEZ-VERA, V., CARDOSO, C., LIU, Q., ELANDER, P. H., DALMAN, K., BEGANOVIC, M., YILMAZ, J. L., MARMON, S., SHABALA, L., SUAREZ, M. F., LJUNG, K., NOVAK, O., SHABALA, S., STYMNE, S., HOFIUS, D. & BOZHKOV, P. V. 2018. Transcriptional stimulation of rate-limiting components of the autophagic pathway improves plant fitness. *J Exp Bot,* 69**,** 1415-1432.

MOSTOWY, S. 2013. Autophagy and bacterial clearance: a not so clear picture. *Cell Microbiol,* 15**,** 395-402.

OHAMA, N., SATO, H., SHINOZAKI, K. & YAMAGUCHI-SHINOZAKI, K. 2017. Transcriptional Regulatory Network of Plant Heat Stress Response. *Trends in Plant Science,* 22**,** 53-65.

PANDEY, P., LEARY, A. Y., TUMTAS, Y., SAVAGE, Z., DAGVADORJ, B., DUGGAN, C., YUEN, E. L., SANGUANKIATTICHAI, N., TAN, E., KHANDARE, V., CONNERTON, A. J., YUNUSOV, T., MADALINSKI, M., MIRKIN, F. G.,

SCHORNACK, S., DAGDAS, Y., KAMOUN, S. & BOZKURT, T. O. 2021. An oomycete effector subverts host vesicle trafficking to channel starvation-induced autophagy to the pathogen interface. *Elife,* 10.

PANDEY, P., RAMEGOWDA, V. & SENTHIL-KUMAR, M. 2015. Shared and unique responses of plants to multiple individual stresses and stress combinations: physiological and molecular mechanisms. *Front Plant Sci,* 6**,** 723.

PATEL, S. & DINESH-KUMAR, S. P. 2008. Arabidopsis ATG6 is required to limit the pathogen-associated cell death response. *Autophagy,* 4**,** 20-7.

PIERETTI, I., ROYER, M., BARBE, V., CARRERE, S., KOEBNIK, R., COULOUX, A., DARRASSE, A., GOUZY, J., JACQUES, M.-A., LAUBER, E., MANCEAU, C., MANGENOT, S., POUSSIER, S., SEGURENS, B., SZUREK, B., VERDIER, V., ARLAT, M., GABRIEL, D. W., ROTT, P. & COCIANCICH, S. 2012. Genomic insights into strategies used by Xanthomonas albilineans with its reduced artillery to spread within sugarcane xylem vessels. *BMC Genomics,* 13.

RAMEGOWDA, V. & SENTHIL-KUMAR, M. 2015. The interactive effects of simultaneous biotic and abiotic stresses on plants: mechanistic understanding from drought and pathogen combination. *J Plant Physiol,* 176**,** 47-54.

RASMUSSEN, S., BARAH, P., SUAREZ-RODRIGUEZ, M. C., BRESSENDORFF, S., FRIIS, P., COSTANTINO, P., BONES, A. M., NIELSEN, H. B. & MUNDY, J. 2013. Transcriptome responses to combinations of stresses in Arabidopsis. *Plant Physiol,* 161**,** 1783-94.

RICO, A. & PRESTON, G. M. 2008. Pseudomonas syringae pv. tomato DC3000 Uses Constitutive and Apoplast-Induced Nutrient Assimilation Pathways to Catabolize Nutrients That Are Abundant in the Tomato Apoplast. *Molecular Plant-Microbe Interactions®,* 21**,** 269-282.

SCHMIDT, A., MÄCHTEL, R., AMMON, A., ENGELSDORF, T., SCHMITZ, J., MAURINO, V. G. & VOLL, L. M. 2019. Reactive oxygen species dosage in Arabidopsis chloroplasts can improve resistance towards Colletotrichum higginsianum by the induction of WRKY33. *New Phytologist,* 226**,** 189-204.

SERTSUVALKUL, N., DEMELL, A. & DINESH-KUMAR, S. P. 2022. The complex roles of autophagy in plant immunity. *FEBS Letters,* 596**,** 2163-2171.

SHARMA, N., CHAUDHARY, C. & KHURANA, P. 2020. Wheat Myo-inositol phosphate synthase influences plant growth and stress responses via ethylene mediated signaling. *Scientific Reports,* 10.

SIGNORELLI, S., TARKOWSKI, Ł. P., VAN DEN ENDE, W. & BASSHAM, D. C. 2019. Linking Autophagy to Abiotic and Biotic Stress Responses. *Trends in Plant Science,* 24**,** 413-430.

SLAVIKOVA, S., UFAZ, S., AVIN-WITTENBERG, T., LEVANONY, H. & GALILI, G. 2008. An autophagy-associated Atg8 protein is involved in the responses of Arabidopsis seedlings to hormonal controls and abiotic stresses. *J Exp Bot,* 59**,** 4029-43.

STEPHANI, M. & DAGDAS, Y. 2020. Plant Selective Autophagy—Still an Uncharted Territory With a Lot of Hidden Gems. *Journal of Molecular Biology,* 432**,** 63-79.

SVENNING, S., LAMARK, T., KRAUSE, K. & JOHANSEN, T. 2011. Plant NBR1 is a selective autophagy substrate and a functional hybrid of the mammalian autophagic adapters NBR1 and p62/SQSTM1. *Autophagy,* 7**,** 993-1010.

THIRUMALAIKUMAR, V. P., GORKA, M., SCHULZ, K., MASCLAUX-DAUBRESSE, C., SAMPATHKUMAR, A., SKIRYCZ, A., VIERSTRA, R. D. & BALAZADEH, S. 2020. Selective autophagy regulates heat stress memory in Arabidopsis by NBR1-mediated targeting of HSP90.1 and ROF1. *Autophagy,* 17**,** 2184-2199.

USTUN, S., HAFREN, A., LIU, Q., MARSHALL, R. S., MININA, E. A., BOZHKOV, P. V., VIERSTRA, R. D. & HOFIUS, D. 2018. Bacteria Exploit Autophagy for Proteasome Degradation and Enhanced Virulence in Plants. *Plant Cell,* 30**,** 668-685.

ÜSTÜN, S., SHEIKH, A., GIMENEZ-IBANEZ, S., JONES, A., NTOUKAKIS, V. & BÖRNKE, F. 2016. The Proteasome Acts as a Hub for Plant Immunity and Is Targeted by Pseudomonas Type III Effectors. *Plant Physiology,* 172**,** 1941-1958.

VAN DOORN, W. G. & PAPINI, A. 2014. Ultrastructure of autophagy in plant cells. *Autophagy,* 9**,** 1922-1936.

WANG, P., NOLAN, T. M., YIN, Y. & BASSHAM, D. C. 2019. Identification of transcription factors that regulate ATG8 expression and autophagy in Arabidopsis. *Autophagy,* 16**,** 123-139.

WANG, Y., BAO, Z., ZHU, Y. & HUA, J. 2009. Analysis of Temperature Modulation of Plant Defense Against Biotrophic Microbes. *Molecular Plant-Microbe Interactions®,* 22**,** 498-506.

WANG, Y., CAI, S., YIN, L., SHI, K., XIA, X., ZHOU, Y., YU, J. & ZHOU, J. 2015. Tomato HsfA1a plays a critical role in plant drought tolerance by activating ATG genes and inducing autophagy. *Autophagy,* 11**,** 2033-2047.

WANG, Y., NISHIMURA, M. T., ZHAO, T. & TANG, D. 2011. ATG2, an autophagy-related protein, negatively affects powdery mildew resistance and mildew-induced cell death in Arabidopsis. *The Plant Journal,* 68**,** 74-87.

WITTE, C. P. 2011. Urea metabolism in plants. *Plant Sci,* 180**,** 431-8.

YAN, Y., WANG, P., HE, C. & SHI, H. 2017. MeWRKY20 and its interacting and activating autophagy-related protein 8 (MeATG8) regulate plant disease resistance in cassava. *Biochem Biophys Res Commun,* 494**,** 20-26.

YANG, Z. & KLIONSKY, D. J. 2009. An Overview of the Molecular Mechanism of Autophagy. *Autophagy in Infection and Immunity.*

YANG, Z. & KLIONSKY, D. J. 2010. Eaten alive: a history of macroautophagy. *Nature Cell Biology,* 12**,** 814-822.

ZESS, E. K., JENSEN, C., CRUZ-MIRELES, N., DE LA CONCEPCION, J. C., SKLENAR, J., STEPHANI, M., IMRE, R., ROITINGER, E., HUGHES, R., BELHAJ, K., MECHTLER, K., MENKE, F. L. H., BOZKURT, T., BANFIELD, M. J., KAMOUN, S., MAQBOOL, A. & DAGDAS, Y. F. 2019. N-terminal β-strand underpins biochemical specialization of an ATG8 isoform. *PLOS Biology,* 17.

ZHANG, B., SHAO, L., WANG, J., ZHANG, Y., GUO, X., PENG, Y., CAO, Y. & LAI, Z. 2020. Phosphorylation of ATG18a by BAK1 suppresses autophagy and attenuates plant resistance against necrotrophic pathogens. *Autophagy,* 17**,** 2093-2110.

ZHANG, H. & SONNEWALD, U. 2017. Differences and commonalities of plant responses to single and combined stresses. *The Plant Journal,* 90**,** 839-855.

ZHENG, Z., QAMAR, S. A., CHEN, Z. & MENGISTE, T. 2006. Arabidopsis WRKY33 transcription factor is required for resistance to necrotrophic fungal pathogens. *The Plant Journal,* 48**,** 592-605.

ZHOU, J., MA, J., YANG, C., ZHU, X., LI, J., ZHENG, X., LI, X., CHEN, S., FENG, L., WANG, P., HO, M. I., MA, W., LIAO, J., LI, F., WANG, C., ZHUANG, X., JIANG, L., KANG, B.-H. & GAO, C. 2023. A non-canonical role of ATG8 in Golgi recovery from heat stress in plants. *Nature Plants,* 9**,** 749-765.

ZHOU, J., PENG, Z., LONG, J., SOSSO, D., LIU, B., EOM, J. S., HUANG, S., LIU, S., VERA CRUZ, C., FROMMER, W. B., WHITE, F. F. & YANG, B. 2015. Gene targeting by the TAL effector PthXo2 reveals cryptic resistance gene for bacterial blight of rice. *The Plant Journal,* 82**,** 632-643.

843 ZHOU, J., WANG, J., CHENG, Y., CHI, Y. J., FAN, B., YU, J. Q. & CHEN, Z. 2013. NBR1-
844 mediated selective autophagy targets insoluble ubiquitinated protein aggregates in plant
845 stress responses. *PLoS Genet,* 9**,** e1003196.
846 ZHOU, J., WANG, J., YU, J. Q. & CHEN, Z. 2014. Role and regulation of autophagy in heat
847 stress responses of tomato plants. *Front Plant Sci,* 5**,** 174.
848 ZHU, J.-K. 2016. Abiotic Stress Signaling and Responses in Plants. *Cell,* 167**,** 313-324.
849 ZHU, T., ZOU, L., LI, Y., YAO, X., XU, F., DENG, X., ZHANG, D. & LIN, H. 2018.
850 Mitochondrial alternative oxidase-dependent autophagy involved in ethylene-mediated
851 drought tolerance in Solanum lycopersicum. *Plant Biotechnology Journal,* 16**,** 2063-
852 2076.

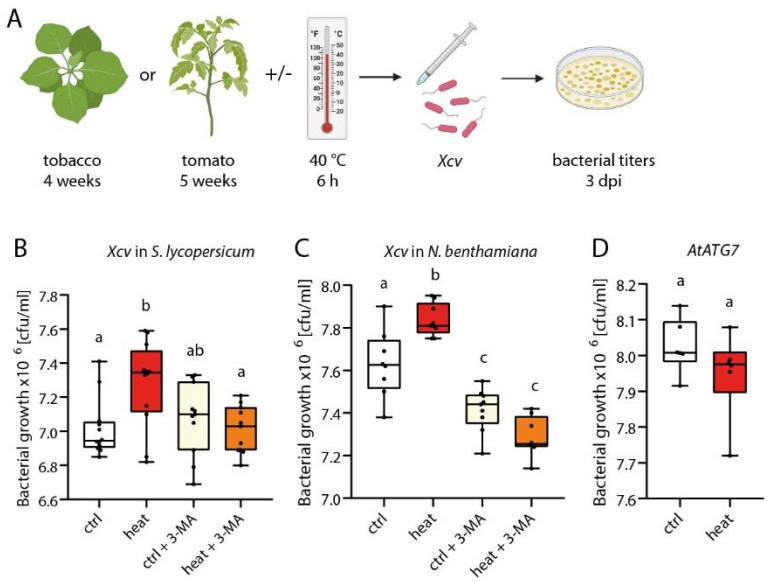

Figure 1: *Xcv* growth is benefited by preceding heat stress in an autophagy-dependent manner. (**A**) Schematic representation of the experimental setup to test bacterial growth in previously heat-stressed plants. (**B,C**) Bacterial growth was tested in tomato (**B)** or tobacco (**C**) plants that were previously subjected to heat or control temperature and co-infiltrated with the autophagy inhibitor 3-MA. (**D**) Bacterial growth in heat- and control-treated tobacco plants transiently expressing *AtATG7*. Experiments were carried out independently at least twice (B)/ three times (C, D) with similar results. Number of biologically independent replicates: *Xcv* in tomato ($n = 12$), *Xcv* in tobacco ($n = 9$), *At*ATG7 ($n = 6$). Statistical analysis was performed by One-way ANOVA and Turkey's multiple comparison test.

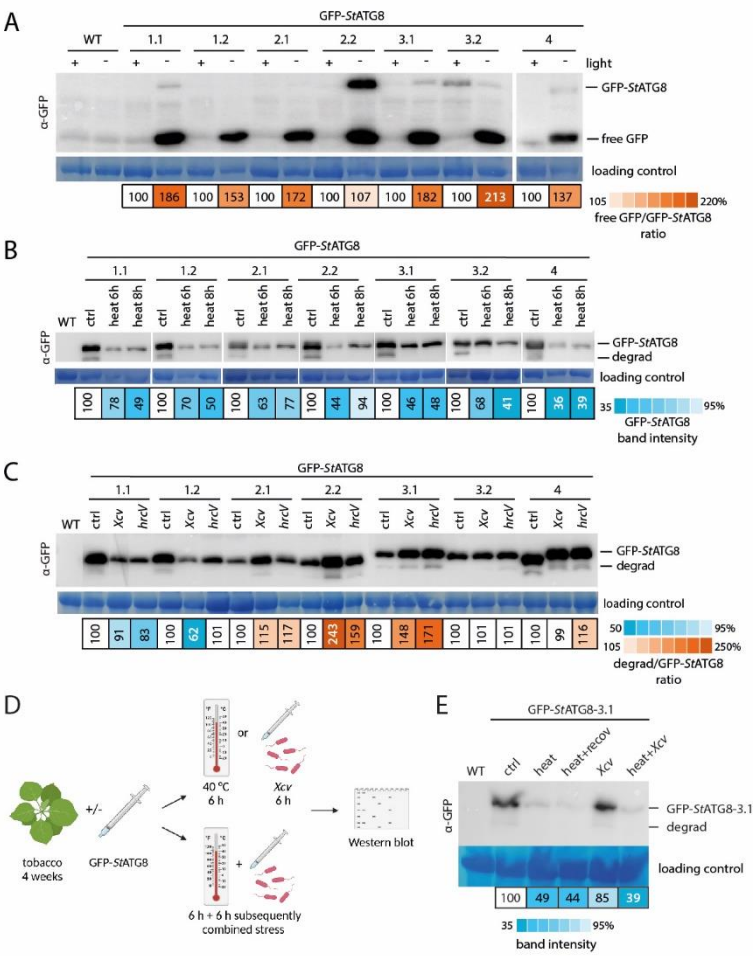

Figure 2: Autophagy is differentially activated under combined stress. (**A-C**) All seven GFP-*St*ATG8 isoforms were transiently expressed in *N. benthamiana*. The plants were subjected to different stresses 1 day after syringe-infiltration of GFP-*St*ATG8 constructs. Western blots show the degradation pattern after 3 days of darkness (**A**), 6/8 h of 40 °C (**B**) and 6 h after *Xcv/hrcV* infection (**C**). Degradation was quantified via measurement of band intensities of GFP-*St*ATG8 (**B**) or GFP-*St*ATG8 and free GFP (**A**) or a specific degradation band (**C**), respectively. (**D**) Schematic representation of the experimental setup to test the effect of combined heat-*Xcv* stress of GFP-*St*ATG8-3.1 degradation and gene expression. (**E**) Degradation pattern of transiently expressed GFP-*St*ATG8-3.1 upon heat, *Xcv,* and a combined heat-*Xcv* challenge. Band intensities were normalized to the protein loading control, and ratios of GFP-*St*ATG8 and a degradation band (if applicable) were calculated. Original blots can be found in the supplemental Fig S3. The experiments were carried out independently three times (B, C, E)/twice (A) with similar results.

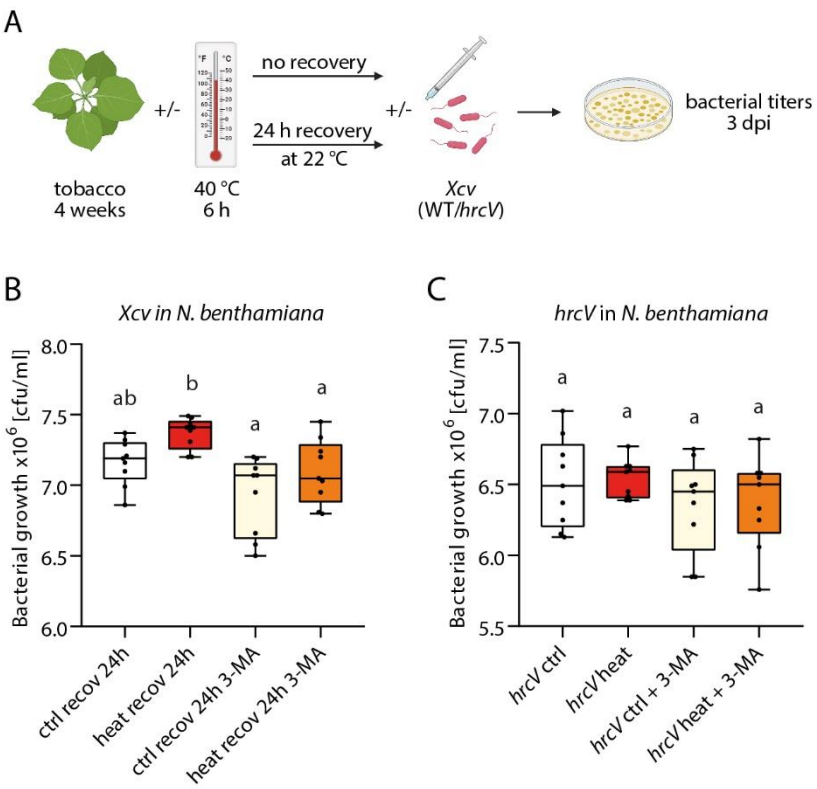

Figure 3: Increased bacterial growth after heat stress is not diminished by a recovery period but is effector-dependent. (**A**) Schematic representation of the experimental setup to test the effect of a recovery phase or effector dependency on bacterial growth. (**B,C**) Bacterial growth of *Xcv* (**B**) or *hrcV* (**C**) was tested in tobacco plants. (**B**) plants were previously subjected to heat or control temperature followed by a 24 h recovery period at control temperature. (**C**) plants were subjected to heat or control conditions followed immediately by bacterial infiltration. In both cases, plants were co-infiltrated with the autophagy inhibitor 3-MA (n = 9 in both experiments). Statistical analysis was performed by One-way ANOVA and Turkey's multiple comparison test.

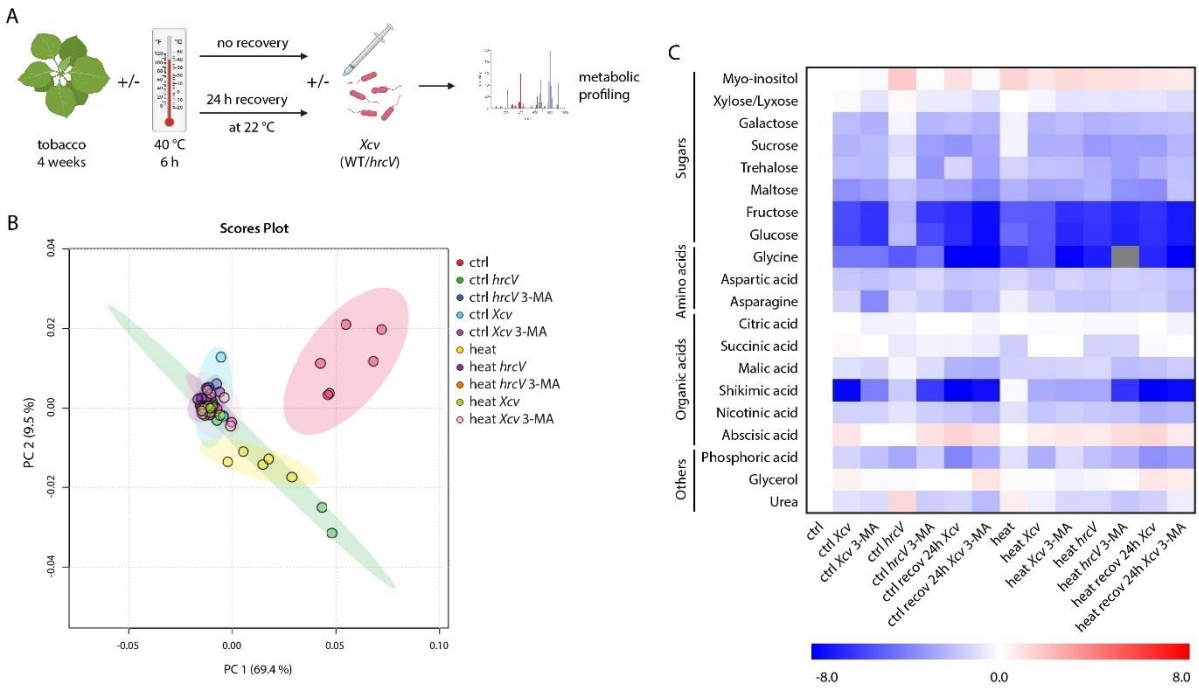

Figure 4: Bacterial infection causes pronounced effects on the plant metabolome. (**A**) Schematic representation of the experimental setup conducted for metabolic profiling. *N. Benthamiana* plants were exposed to heat stress with/without a 24 h recovery period, then infiltrated by *Xcv/hrcV* and co-infiltrated with the autophagy inhibitor 3-MA. Samples were collected for metabolic profiling by GC-MS 3 d post-infection (n=5-6). (**B**) Principal component analysis of the metabolome in response to heat treatment or bacterial infection with and without a recovery phase and 3-MA treatment. (**C**) Heat maps displaying median values in log2 scale of the response of 4 different groups of metabolites to stress treatment as in (A). Red color refers to upregulation compared to the control; blue color refers to downregulation compared to the control.

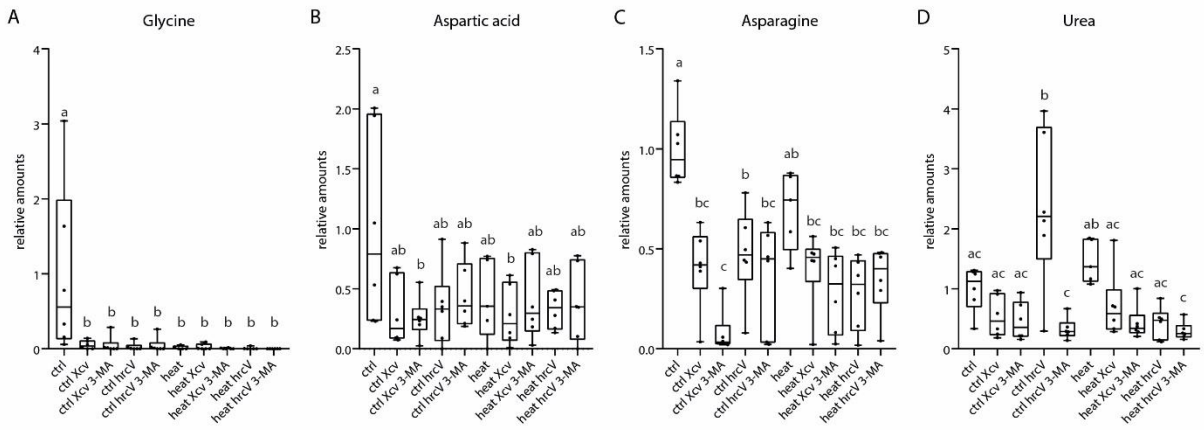

Figure 5: Detailed overview of effects of *Xcv* infection on the levels of three amino acids and urea. Boxplots showing levels of Glycine (**A**), Aspartic acid (**B**), Asparagine (**C**), and urea (**D**) in response to *Xcv*, *hrcV*, and heat treatment, respectively (n = 5-6). Statistical analysis was performed by One-way ANOVA and Turkey's multiple comparison test.

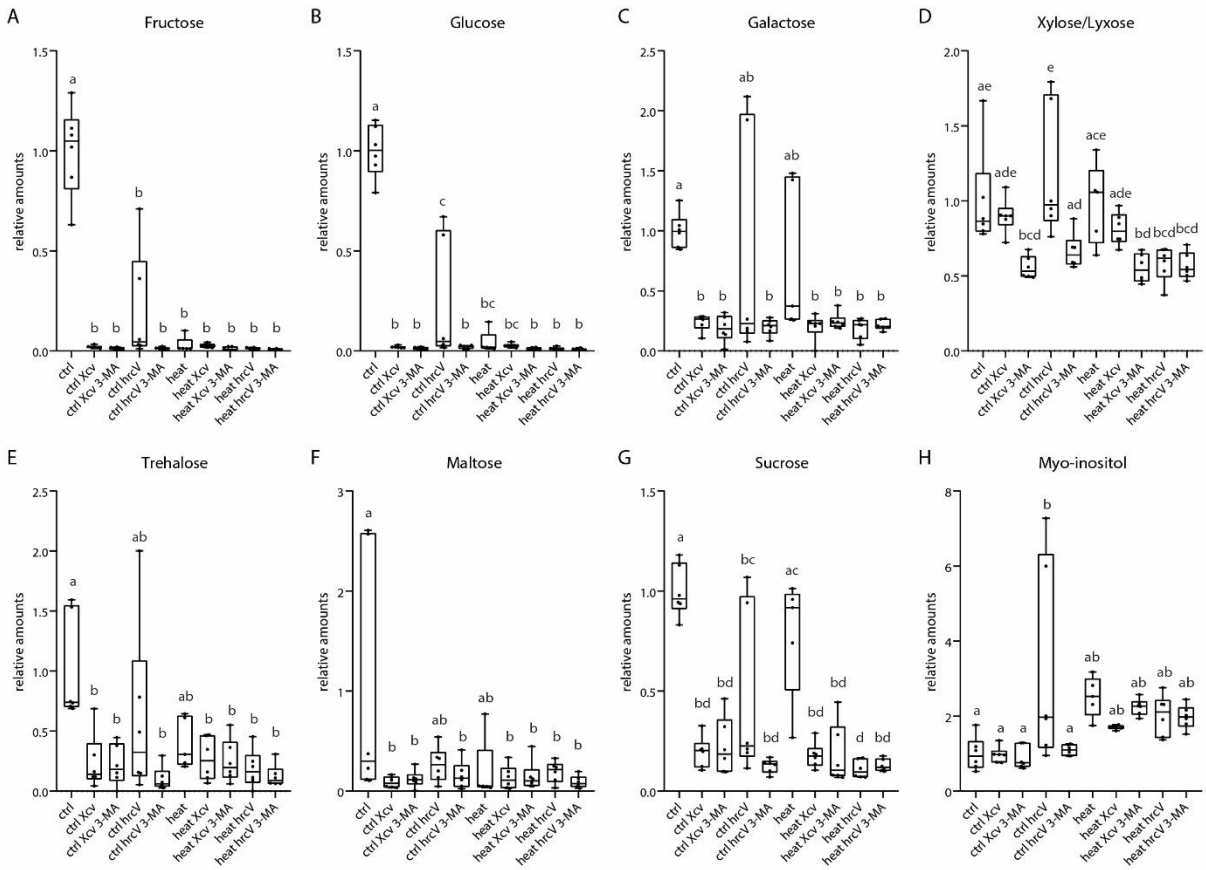

Figure 6: Detailed overview of effector-dependent effects of *Xcv* infection on sugar levels. Boxplots showing levels of (**A-D**) Mono-, (**E-G**) Disaccharides, and (**H**) sugar alcohol in response to *Xcv*, *hrcV*, and heat treatment, respectively (n = 5-6). Statistical analysis was performed by One-way ANOVA and Turkey's multiple comparison test.

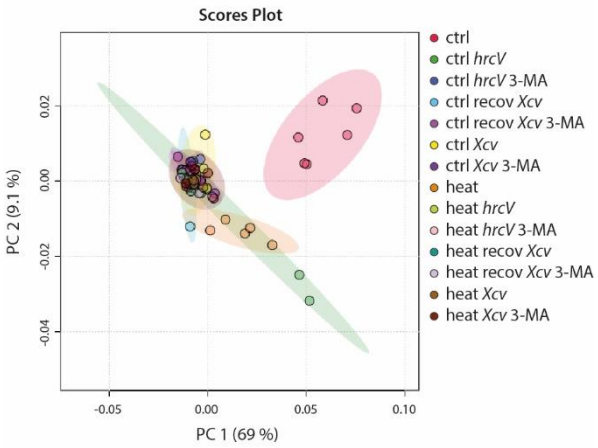

Supplemental Figure S1: Principal component analysis of the metabolome as in Figure4B including heat recovery samples

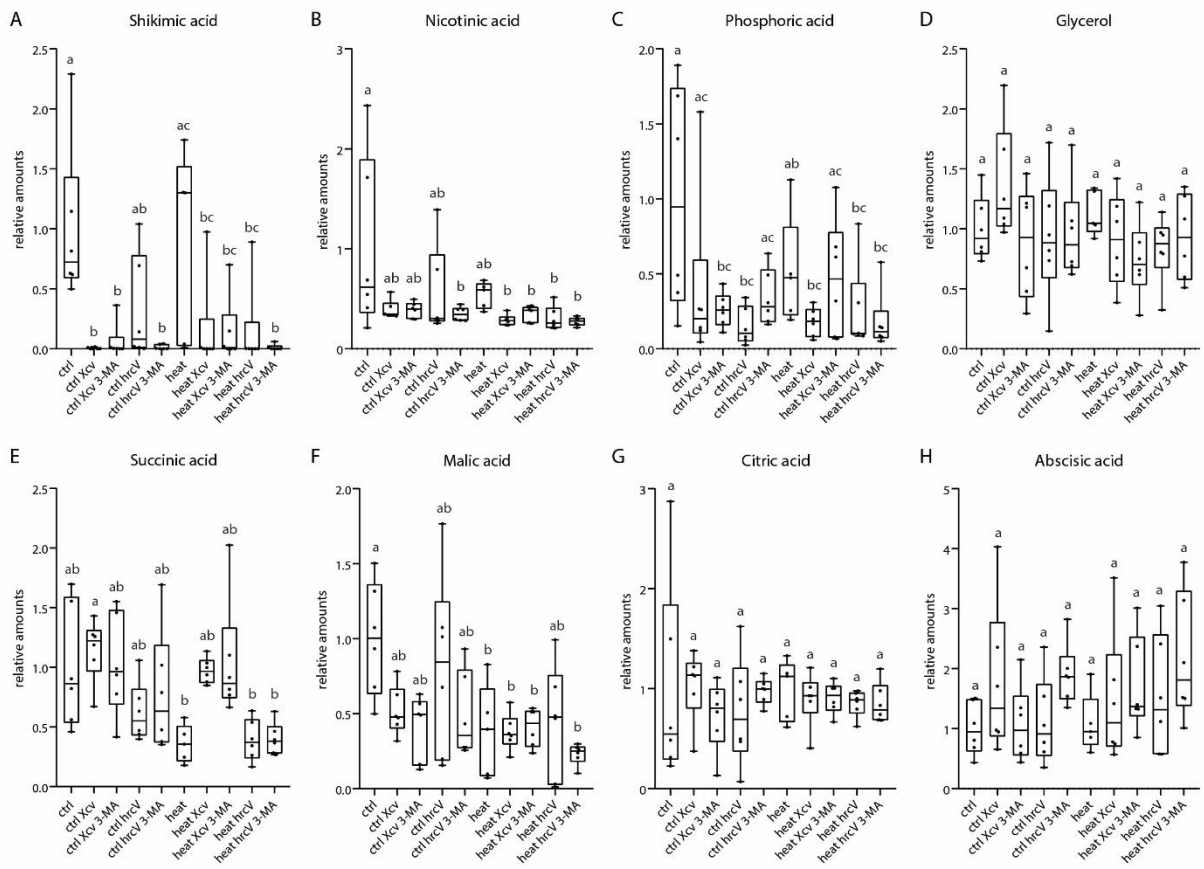

Supplemental Figure S2: Detailed overview on effects of *Xcv* infection and heat on the levels of organic compounds. Boxplots showing levels of Shikimic acid (**A**), Nicotinic acid (**B**), Phosphoric acid (**C**), Glycerol (**D**), Succinic acid (**E**), Malic acid (**F**) Citric acid (**G**), and Abscisic acid (**H**) in response to *Xcv*, *hrcV*, and heat treatment, respectively (n = 5-6). Statistical analysis was performed by One-way ANOVA and Turkey's multiple comparison test.

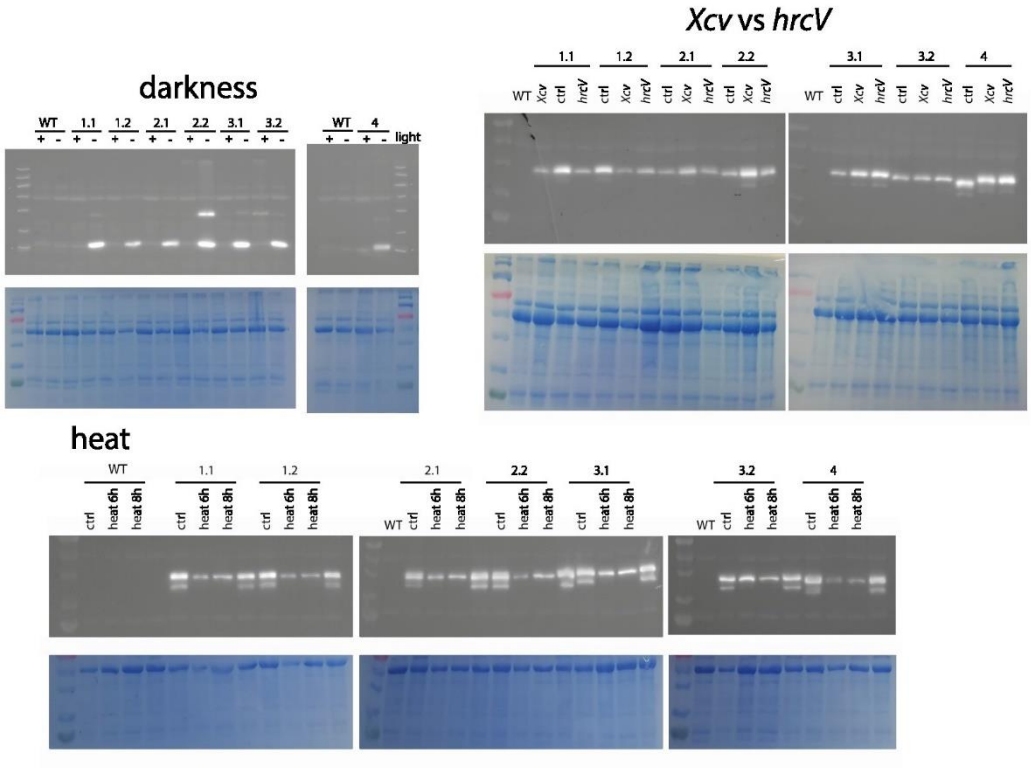

925

926 **Supplemental Figure S3:** Original blots depicted in Figure 2

927

928

929